

# Highly Integrated Optical $4 \times 4$ Crossbar in Silicon-on-Insulator Technology

Andrzej Kaźmierczak, Wim Bogaerts, *Member, IEEE*, Emmanuel Drouard, Fabian Dortu, Pedro Rojo-Romeo, Frederic Gaffiot, Dries Van Thourhout, and Domenico Giannone

**Abstract**—In this paper, we present the design, fabrication, and characterization of a highly integrated optical  $4 \times 4$  crossbar based on microring resonator add-drop filters. The designed crossbar structure, as small as  $50 \mu\text{m} \times 50 \mu\text{m}$ , has been fabricated in CMOS compatible silicon on insulator technology. Finally, experimental results proving the proper operation of the fabricated crossbar structures are discussed.

**Index Terms**—Add-drop filters, optical crossbar, optical microring resonators optical on chip interconnections.

## I. INTRODUCTION

THE technology for fabricating integrated circuits (ICs) has improved to such a level that fabricating chips with more than one billion transistors has become feasible. It is predicted that in the near future electrical intra- or interchip communication between such large numbers of transistors will constitute a major bottleneck of further IC performance development [1]. In the case of intrachip communication, the expected constraints are expressed in terms of power consumption and latency [2] while in the case of interchip interconnections the bandwidth is the limiting factor [3]. Optical on-chip communication is one of the solutions currently being investigated for addressing these problems [4]. The proposed design of an optical crossbar enables high-bandwidth and low-contention data routing through wavelength multiplexing.

## II. OPTICAL CROSSBAR BASICS

The optical crossbar concept was proposed by O'Connor [5]. An optical crossbar is a passive waveguiding structure that enables bidirectional optical communication between a certain number of input and output ports. In the case of on-chip interconnects these ports should be connected to major IP

Manuscript received July 04, 2008; revised October 20, 2008. First published April 17, 2009; current version published July 24, 2009.

A. Kaźmierczak, F. Dortu, and D. Giannone are with the Applied Photonics Department, Multitel a.s.b.l., Mons, B-7000 Belgium (e-mail: andrzej.kaźmierczak@multitel.be; fabian.dortu@multitel.be and domenico.giannone@multitel.be).

W. Bogaerts and D. Van Thourhout are with the Ghent University—Interuniversity Microelectronics Center (IMEC), Department of Information Technology, Gent 9000, Belgium (e-mail: wim.bogaerts@ugent.be; dries.vanthourhout@intec.ugent.be).

E. Drouard, P. Rojo-Romeo, and F. Gaffiot are with the Institut des Nanotechnologies de Lyon, Université de Lyon, INL-UMR5270, CNRS, Ecole Centrale de Lyon, F-69134 Ecully, France (e-mail: emmanuel.drouard@ec-lyon.fr; pedro.rojo-romeo@ec-lyon.fr; frederic.gaffiot@ec-lyon.fr).

Color versions of one or more of the figures in this paper are available online at <http://ieeexplore.ieee.org>.

Digital Object Identifier 10.1109/JLT.2008.2010462

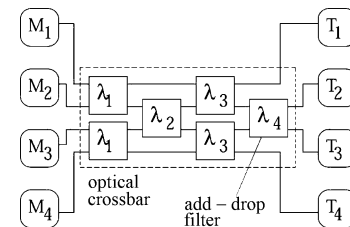


Fig. 1. Schematic of  $4 \times 4$  optical network on chip.

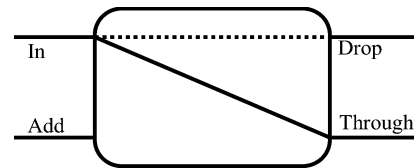


Fig. 2. Black-box representation of the optical add-drop filter in the crossbar.

blocks (e.g., processor cores, memory blocks, functional units, etc.) of an IC to provide an optical link between these blocks. A simplified schematic of the proposed communication scheme, called an optical network on chip (ONoC), is shown in Fig. 1.

The M and T symbols correspond to masters and targets (we suppose the IP blocks are equipped with optoelectronics transceivers, outside of the scope of this paper). The IP blocks are connected to the optical crossbar: a fully passive, wavelength-routed optical network constituting the core of the ONoC. As the crossbar is designed for on-chip communication it has to be bidirectional. The crossbar is composed of wideband waveguide structures and four rows of wavelength selective components (add-drop filters). In the present example, a  $4 \times 4$  crossbar is shown, though it can be expanded to other configurations, e.g.,  $16 \times 16$ , by the simple addition of more add-drop filters rows. In order to provide wavelength routing from each master to all targets and from each target to all masters, a specific design for the add-drop filters is required, where the nonresonant signal propagates in diagonal direction, whereas the resonant one is dropped forward in straight direction. A black-box representation of such filter is shown in Fig. 2.

The use of a line of such configured add-drop filters enables optical signal routing from one input port to numerous out ports. When they are configured in a network (e.g., like in Fig. 1), it permits communication between each of the masters to each of the targets and vice versa. The operation of the network is depicted in Table I.

From the table one can see that with a set of four wavelengths (corresponding to the resonant wavelengths of the add-drop filters in the network) it is possible to establish a communication

TABLE I  
OPERATION TRUTH TABLE OF THE  $4 \times 4$  OPTICAL CROSSBAR

|    | T1           | T2           | T3           | T4           |
|----|--------------|--------------|--------------|--------------|
| M1 | $\lambda_2$  | $\lambda_3$  | $\lambda_1$  | Non resonant |
| M2 | $\lambda_3$  | $\lambda_4$  | Non resonant | $\lambda_1$  |
| M3 | $\lambda_1$  | Non resonant | $\lambda_4$  | $\lambda_3$  |
| M4 | Non resonant | $\lambda_1$  | $\lambda_3$  | $\lambda_2$  |

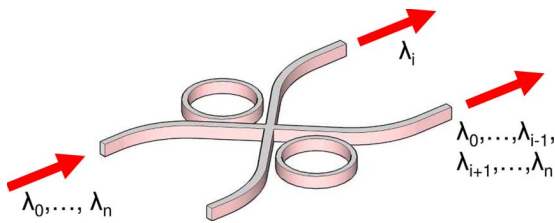


Fig. 3. Principles of the optical add-drop filter based on waveguide intersections.

path between all master and target ports. For the communication from a particular port, three add-drop filter rows are acting as switches and the wavelength corresponding to the remaining filter acts as a nonresonant wavelength. When expanding the optical crossbar the table can be expanded analogously.

### III. THE OPTICAL ADD-DROP FILTER

The use of microring resonators allows building compact and efficient wavelength switching devices. Using silicon on insulator (SOI) CMOS compatible technology, it is possible to fabricate compact ring resonators structures with resonator radii as small as  $1.5 \mu\text{m}$  [6]. In the classical form, this type of filter is composed of two parallel bus waveguides coupled by a microring. Unfortunately, this configuration reverses the direction of the dropped signal, introducing the need for complicated waveguide topology or resonator pairs [7]. To avoid these problems, we propose an add-drop filter configuration based on a waveguide intersection [8]–[10] with a pair of small size (radii as small as  $2 \mu\text{m}$ ) side coupled microring resonators as shown in Fig. 3.

The choice of this type of wavelength routing device, using two ring resonators, was encouraged by the study of Little [11] and Klein [12], who first fabricated optical  $1 \times 4$  and  $1 \times 8$  networks based on add-drop filters with a single ring resonator and a waveguide intersection, of much larger dimensions however (ring diameter of  $100 \mu\text{m}$ ). The add-drop filter configuration proposed in this paper has several important advantages:

- Central symmetry leading to exactly the same properties independent of the injection port.
- Simple waveguide layout with a small occupied chip area which is a substantial requirement for on-chip communications.

The presence of a waveguide crossing may be seen as a disadvantage of the chosen topology leading to additional

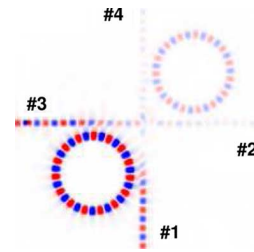


Fig. 4. 3-D FDTD simulation of the electromagnetic field distribution in the add-drop filter.

signal losses and crosstalk. It is however unavoidable in order to achieve the requested signal routing [13], but, if needed, the crosstalk can be reduced by introducing an improved waveguide crossing layout [14].

Alternative techniques, such as arrayed waveguide grating routers (AWG), [15] typically have a much larger footprint than the device discussed here, and are therefore not as attractive for densely packed on-chip optical interconnects.

### IV. ADD-DROP FILTERS DESIGN AND SIMULATION

In order to evaluate the concept of the proposed add-drop filter, test structures were designed, fabricated, and characterized experimentally. The structures were designed for the IMEC photonic wire technology in SOI substrate [16]. The waveguide height is fixed to  $220 \text{ nm}$  and the width is  $450 \text{ nm}$ . In the coupling sections the coupling between the bus waveguide and the resonator is improved by reducing the waveguide width to  $350 \text{ nm}$ . The coupling gap between resonators and waveguides is set to  $200 \text{ nm}$  and four resonators radii,  $1.8$ ,  $1.9$ ,  $2.0$ , and  $2.1 \mu\text{m}$ , respectively, are considered.

The designed filter structure has been validated using three-dimensional finite-difference time domain (3-D FDTD) simulations. In Fig. 4, a 3-D FDTD simulation of the electromagnetic field, at resonance, in the add-drop filter with a  $2.1 \mu\text{m}$  resonator radius is shown.

The proper signal dropping is demonstrated, since the light injected to the port #1 is almost completely dropped to port #3. This is further confirmed by the transmission spectrum in Fig. 5, showing that depending on the wavelength, light is either transmitted to port #4 or dropped to port #3. The transmission to port #2 (crosstalk) is as small as  $-15 \text{ dB}$ . In the wavelength range  $1500$ – $1580 \text{ nm}$ , resonant peaks are present at  $1521.00$  and  $1568.05 \text{ nm}$ , from which we derive a free spectral range (FSR) of  $47.05 \text{ nm}$ . The resonant peaks are rather sharp with a quality factor ( $Q$ ) reaching  $1000$ . Both the dropping efficiency and the nonresonant efficiency are close to  $80\%$ .

### V. CHARACTERIZATION OF ADD-DROP FILTERS

The fabricated structures were fabricated using deep UV lithography on SOI substrates [16], with dimensions as described above. In Fig. 6, SEM micrograph of fabricated add-drop filter structure is shown.

In order to increase the coupling efficiency without deteriorating the transmission properties of the waveguides,  $30^\circ$  angled coupling waveguide sections, wrapping around the resonator, were introduced. The test structures were equipped with surface

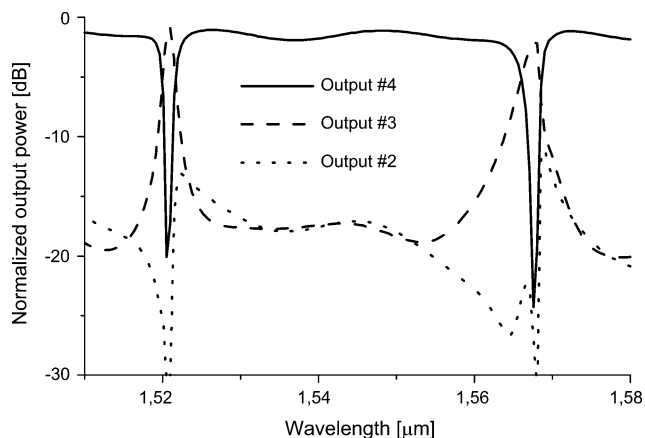


Fig. 5. 3-D FDTD simulation of the add-drop filter transmission spectrum.

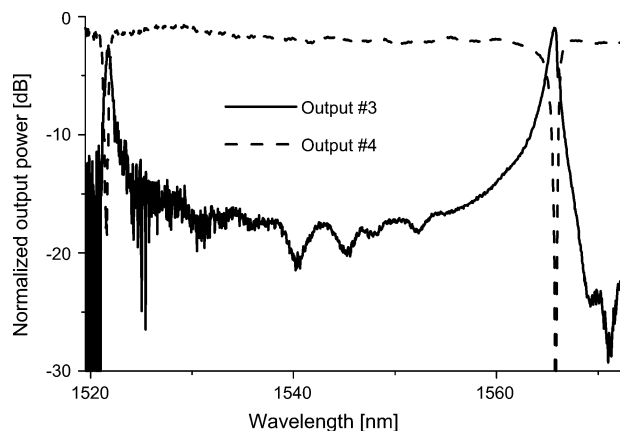


Fig. 7. Wavelength transmission spectrum of the add-drop filter with the resonators radii of 1.9  $\mu\text{m}$ .

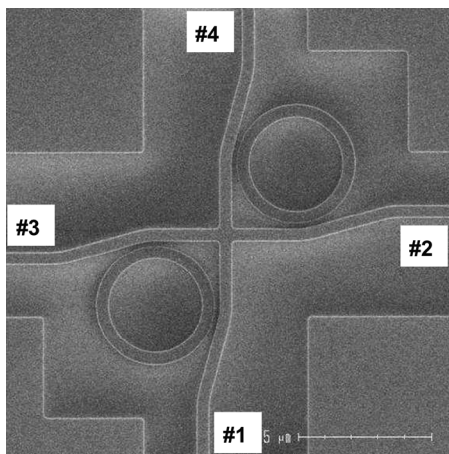


Fig. 6. SEM micrograph of the fabricated add-drop filter test structure.

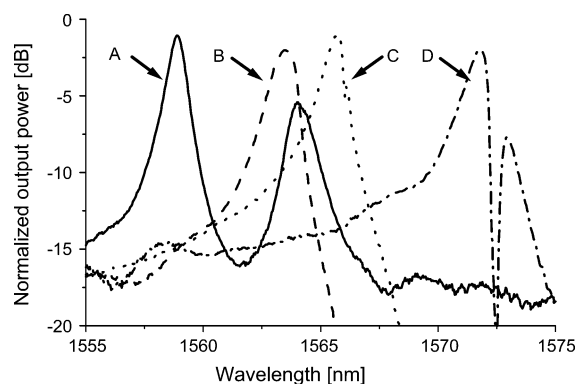


Fig. 8. Resonance peaks of filters with resonators radii of 2.1  $\mu\text{m}$  (A), 2.0  $\mu\text{m}$  (B), 1.9  $\mu\text{m}$  (C), and 1.8  $\mu\text{m}$  (D).

grating couplers at the inputs and outputs of the bus waveguides setting the polarization state within the bus waveguides to TE [17].

The fabricated structures were evaluated experimentally by measuring the transmission of a broadband near infrared response light source with an optical spectrum analyzer. The obtained transmission spectra were normalized to the transmission spectrum of a straight waveguide of same optical path length, therefore removing the wavelength-dependence of the input grating insertion loss. The resulting spectrum is shown in Fig. 7.

In the wavelength range 1515–1575 nm, two resonant peaks are present, at 1521.76 and 1565.72 nm, yielding a FSR of 43.96 nm. The resonant peak at 1565.72 nm is sharp and high with a quality factor of 1700 and a normalized dropped signal level of 0.81, which is actually higher than the nonresonant transmission level (0.70).

Similar measurements were conducted for filters with different resonator radii. The transmission spectra of the dropped signals (at port #3) are depicted in Fig. 8.

As expected, the shift of the resonators radii causes a shift in the resonant frequency. A 100 nm increase in resonator radius shifts the resonant wavelength by a value between 2.28

and 6.12 nm. This indicates a slight difference in radius between the designed and the fabricated resonators. Nonetheless, it is still possible to produce four well-separated resonant peaks. Note that the normalized dropped signal transmission is high, reaching up to 81% in the best case and above 63% for all channels. It is also noticeable that in the case of peaks A (of 2.1  $\mu\text{m}$  resonators radii device) and D (1.8  $\mu\text{m}$  radii) double resonant peaks appear. The origin of these peaks seems to be different. The peaks of larger resonator seems to be a zero and first radial order modes (similarly to the one obtained in [8]), while the double-peak of ring resonators with 1.8  $\mu\text{m}$  is probably originating from slight difference of resonators properties (e.g., radii) of this filter. One can also observe that the quality factor of the filter with ring resonators radii of 2.0  $\mu\text{m}$  is significantly lower than for the other filters. This is probably due to random fabrication problems leading to high attenuation in the rings (e.g., problems with coupling section).

The obtained results in terms of resonant wavelength ( $\lambda_{\text{RES}}$ ), FSR, resonance peak quality factor ( $Q$ ), and normalized level of dropped signal (D) are summarized in Table II.

## VI. OPTICAL CROSSBAR DESIGN AND SIMULATION

The experimental characteristics of proposed add-drop filters shown in the previous section were encouraging enough to design and fabricate an optical crossbar based on such add-drop

TABLE II  
COMPARISON OF THE EXPERIMENTAL RESULTS OBTAINED FOR ADD-DROP  
FILTERS WITH DIFFERENT RESONATORS RADII (R)

| R[ $\mu\text{m}$ ] | $\lambda_{\text{RES}}$ [nm] | FSR [nm] | Q    | D    |
|--------------------|-----------------------------|----------|------|------|
| 2.1                | 1558.84                     | 39.88    | 1770 | 0.78 |
| 2.0                | 1563.44                     | 41.72    | 760  | 0.63 |
| 1.9                | 1565.72                     | 43.96    | 1700 | 0.81 |
| 1.8                | 1571.84                     | 46.68    | 1389 | 0.63 |

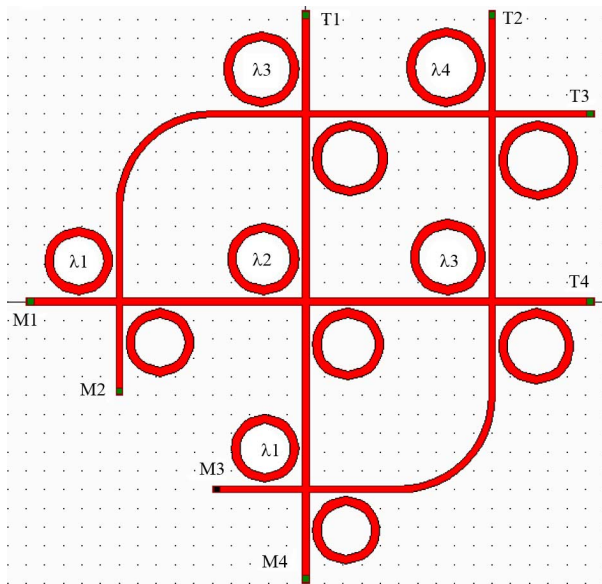


Fig. 9. Topology of the  $4 \times 4$  optical crossbar.

filters. With four add-drop filters of different resonators radii, it is possible to design an optical  $4 \times 4$  crossbar as shown in Fig. 9.

The crossbar is composed of four rows of add-drop filters with different resonators radii, namely  $\lambda_1 = 1.8$ ,  $\lambda_2 = 1.9$ ,  $\lambda_3 = 2.0$ , and  $\lambda_4 = 2.1 \mu\text{m}$ . The proposed topology is very compact as it occupies an area smaller than  $50 \times 50 \mu\text{m}^2$ . The parameters of the filters (e.g., waveguides height, width, etc.) are the same as the previously evaluated stand-alone devices. The operation of the crossbar was simulated using 2-D FDTD code. The simulated transmission spectrum at ports T1–T4 with light injected to port M2 is shown in Fig. 10.

As expected from Table I, Fig. 10 shows three resonant peaks corresponding to light at  $\lambda_3$ ,  $\lambda_4$ , and  $\lambda_1$  ( $\pm$  an integer multiple of the FSR) dropped respectively to ports T1, T2, and T4, while the light at nonresonant wavelengths is transmitted to port T3. The resonant peaks are reasonably well separated demonstrating the possibility to address all output ports by changing the transmitter wavelength. The operational principle of the optical crossbar is therefore proved.

## VII. CHARACTERIZATION OF THE OPTICAL CROSSBAR

The designed optical  $4 \times 4$  crossbar has been fabricated using the process described in Section V.

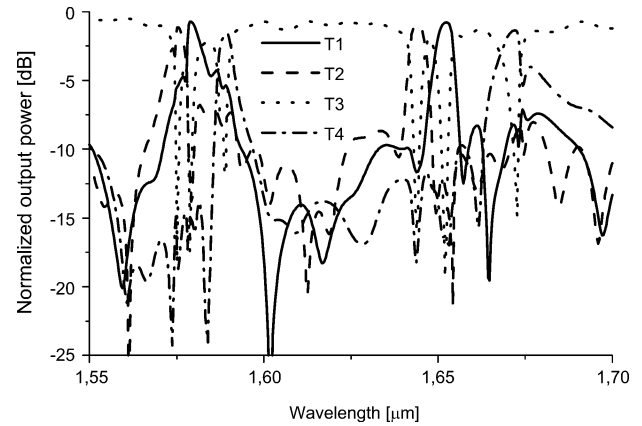


Fig. 10. Simulated transmission spectrum of the optical  $4 \times 4$  crossbar at ports T1 to T4, with the light injected at the port M2.

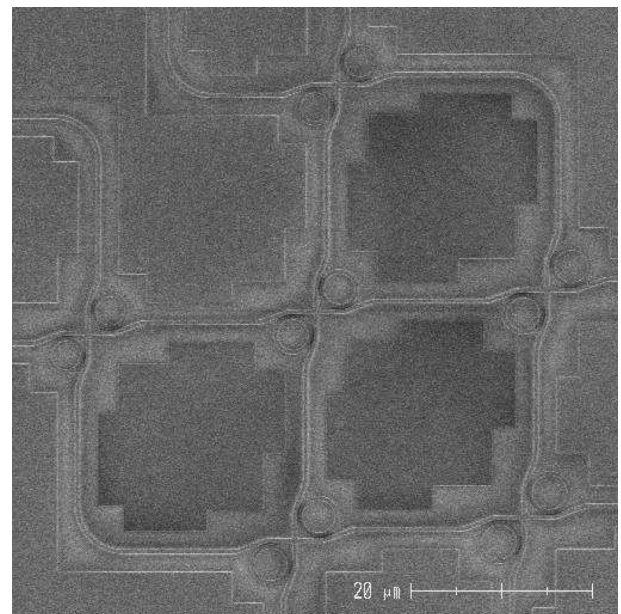


Fig. 11. SEM micrograph of the fabricated optical  $4 \times 4$  crossbar structure.

The fabricated structure shown on the SEM micrograph of Fig. 11 has the same composition as the simulated structure of Fig. 9 and was characterized in a similar way as described in Section V.

The transmission spectrum of the crossbar in Fig. 12 shows two groups of resonant peaks around 1530 and 1570 nm, reflecting the FSR of the filters which is about 40 nm. The transmitted normalized signal is relatively low ( $\sim 20\%$ ). The losses mainly originate from the waveguide crossings. In the close-up of the transmission spectrum shown in logarithmic scale in Fig. 13, we see that the crosstalk between the dropped signals and nonresonant transmission is rather weak and do not exceed  $-20$  dB, which corresponds to less than 6% of the normalized nonresonant transmission. However, the crosstalk between some dropped channels is larger ( $-7.5$  dB to the channel T1 at the first transmission peak), this inconvenience can be resolved by separating resonant peaks along the whole FSR. Nonetheless, resonant peaks are well separated so that addressing each output port is possible.

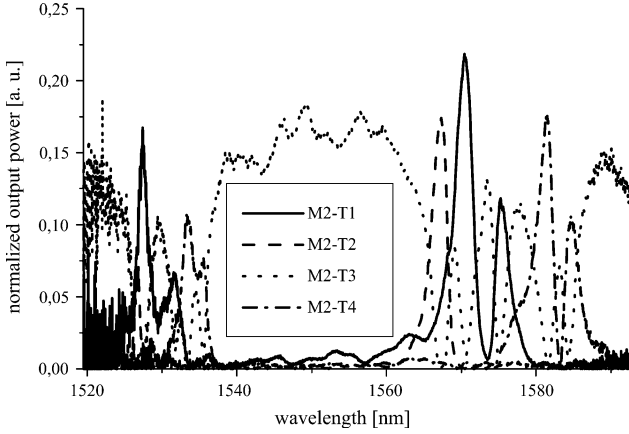


Fig. 12. Measured transmission spectrum of the optical 4 × 4 crossbar at ports T1 T4 with light injected at port M2.

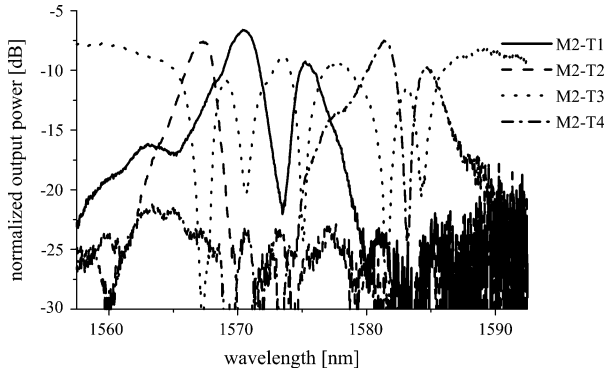


Fig. 13. Close-up of the measured transmission spectrum of the optical 4 × 4 crossbar at ports T1 T4 with light injected at port M2.

The three resonant peaks at 1567.32, 1570.52, and 1581.40 nm correspond to light dropped to ports T1, T2, and T4 by filters  $\lambda_3$ ,  $\lambda_4$ , and  $\lambda_1$ , respectively. The measured quality factors range between 590 and 720. One sees that the peaks at 1570.52 nm (T1) and 1581.40 nm (T4) are split in two. This is probably due to a slight difference in the radii of the ring resonator pair of the corresponding add-drop filters ( $\lambda_3$  and  $\lambda_1$ , respectively, for T1 and T4). The dependence of resonant wavelength on resonator geometry is given by commonly known resonance condition

$$m\lambda_{\text{RES}} = n_{\text{eff}}L \quad (1)$$

where  $m$  is an integer,  $\lambda_{\text{RES}}$  is a resonant wavelength,  $n_{\text{eff}}$  is the effective index of the mode and  $L$  is the resonator length. Therefore, the resonance shift caused by radius imperfection can be written as

$$\frac{\Delta\lambda_{\text{RES}}}{\lambda_{\text{RES}}} = \frac{\Delta R}{R} \quad (2)$$

where  $R$  is the resonator radius. The resonant wavelength shift due to effective index change can be given as

$$\frac{\Delta\lambda_{\text{RES}}}{\lambda_{\text{RES}}} = \frac{\Delta n_{\text{eff}}}{n_{\text{eff}}} \quad (3)$$

TABLE III  
OPERATION TRUTH TABLE OF THE OPTICAL 4 × 4 CROSSBAR TEST STRUCTURE

|    | T1           | T2           | T3           | T4           |
|----|--------------|--------------|--------------|--------------|
| M1 | 1571.92      | 1572.28      | 1581.32      | Non resonant |
| M2 | 1570.52      | 1567.32      | Non resonant | 1581.40      |
| M3 | 1580.96      | Non resonant | 1566.80      | 1573.36      |
| M4 | Non resonant | 1580.84      | 1570.36      | 1571.68      |

TABLE IV  
EXPERIMENTAL CROSSTALK VALUES FOR THE SIGNAL INJECTED AT PORT M2

| Destination port/<br>$\lambda$ [nm] | Crosstalk to T1<br>[dB] | Crosstalk to T2<br>[dB] | Crosstalk to T3<br>[dB] | Crosstalk to T4<br>[dB] |
|-------------------------------------|-------------------------|-------------------------|-------------------------|-------------------------|
| T1/<br>1570.52                      |                         | -24,68                  | -9,99dB                 | -18,00                  |
| T2/<br>1567.32                      | -5,18                   |                         | -16,75                  | -16,02                  |
| T3/<br>1573.50                      | -9,93                   | -15,75                  |                         | -17,93                  |
| T4/<br>1581.40                      | -16,30                  | -20,47                  | -12,35                  |                         |

This leads to the conclusion that resonator radius and width (as influencing effective index) fabrication precision, at least as good as single nanometer, is required in order to provide the resonant wavelength precision as good as 1 nm. For the practical application, it might be profitable to introduce integrated heaters onto the ring resonators in order to compensate technological imperfections. This would be a further step in our research on development of these devices. A similar measurement was performed for all input ports of the network. The results are summarized in Table III.

This table demonstrates that communication between all input and output ports of the network can be established. Furthermore, choosing the proper wavelength allows each output port to be addressed. Some slight differences between filters of the same switching row causes appearance of more than four resonant wavelengths in the table. This problem can be minimized by technology improvement leading to higher resonators uniformity.

As the characterized structure is the first prototype of such interconnection network, the design was not fully optimized yet (e.g., by equally spacing resonant peaks along the spectral range). Thus, significant crosstalk level occurred. Example of crosstalk calculations is shown in Table IV.

The table shows the experimental values of crosstalk for the signal injected to port M2 that corresponds to the spectrum shown in Fig. 13. The crosstalk was calculated as the difference between the power at the destination signal and power collected at other outputs. The calculation was made at resonant wavelengths shown in Table III (for nonresonant transmission

to port T3 for the wavelength of 1573.50 nm) with the realistic bandwidth of 0.8 nm that corresponds to the bandwidth of DWDM systems. As one sees the crosstalk is usually smaller than  $-10$  dB. The exceptional case of crosstalk between ports T1 and T2 at the wavelength of 1567.32 nm is caused by the overlapping of two neighboring resonant peaks as it is clearly visible in the spectrum. This could be avoided with further optimization leading to use of the complete spectral range of the photonic circuit.

## VIII. CONCLUSION

In this paper we presented the design, fabrication, and characterization of highly compact add-drop filters based on microring resonators and waveguides intersection. The designed devices exploit submicrons waveguides and ring resonators with radii as small as  $1.8 \mu\text{m}$ . The structures have been fabricated on a SOI substrate using deep UV lithography. The experimental transmission spectra have demonstrated the proper operation of the add-drop filters and their suitability to be used in an optical crossbar.

Consequently, we proposed the design, fabrication and characterization of a highly integrated optical  $4 \times 4$  crossbar. Presented network exhibits fully bidirectional transmission between four input and four output ports.

Furthermore, the optical crossbar occupies area as small as  $50 \mu\text{m} \times 50 \mu\text{m}$ , which is the smallest reported value for this type of networks.

The transmission spectra measurements demonstrate the proper operation of the crossbar though signal losses are rather high. Further development including waveguide crossing optimization and introduction of active adjustment of resonator properties should allow improving the signal in terms of signal losses, to obtain better resonator uniformity and to integrate more channels (e.g.,  $12 \times 12$  or  $16 \times 16$ ).

## REFERENCES

- [1] *International Technology Roadmap for Semiconductors*. : Semiconductor Industry Association, San Jose, CA, 2005.
- [2] G. Tosik, F. Gaffiot, Z. Lisik, I. O'Connor, and F. Tissafi-Drissi, "Power dissipation in optical and metallic clock distribution networks in new VLSI technologies," *Proc. Inst. Electr. Eng. Electr. Lett.*, vol. 4, no. 3, 2004.
- [3] D. A. B. Miller, "Rationale and challenges for optical interconnects to electronic chips," *Proc. IEEE*, vol. 88, p. 728, June 2000.
- [4] M. J. McFadden, M. Iqbal, T. Dillon, R. Nair, T. Gu, D. W. Prather, and M. W. Haney, "Multiscale free-space optical interconnects for intrachip global communication: Motivation, analysis, and experimental validation," *Appl. Opt.*, vol. 45, pp. 6358–6366, 2006.
- [5] I. O'Connor and F. Gaffiot, "On-chip optical interconnect for low-power," in *Ultra Low-Power Electronics and Design*, E. Macii, Ed. Dordrecht, Germany: Kluwer, 2004, pp. 1–20.
- [6] P. Dumon, W. Bogaerts, V. Wiaux, J. Wouters, S. Beckx, J. Van Campenhout, D. Taillaert, B. Luyssaert, P. Bienstman, D. Van Thourhout, and R. Baets, "Low-loss SOI photonic wires and ring resonators fabricated with deep UV lithography," *IEEE Photon. Technol. Lett.*, vol. 16, no. 5, pp. 1328–1330, May 2004.
- [7] A. Kazmierczak, M. Briere, E. Drouard, P. Rojo-Romeo, I. O'Connor, X. Letartre, F. Gaffiot, L. El Melhaoui, P. Lyan, and J. M. Fedeli, "Design and characterisation of optical networks on chip," in *Proc. 12th European Conference on Integrated Optics ECIO '05.*, Grenoble, 2005, pp. 188–191.

- [8] A. Kazmierczak, M. Briere, E. Drouard, P. Bontoux, P. Rojo-Romeo, I. O'Connor, X. Letartre, F. Gaffiot, R. Orobtcchouk, and T. Benyattou, "Design, simulation and characterization of a passive optical add-drop filter in silicon-on-insulator technology," *IEEE Photon. Technol. Lett.*, vol. 17, no. 7, pp. 1447–1449, July 2005.
- [9] F. Xu and A. W. Poon, "Silicon cross-connect filters using microring resonator coupled multimode-interference-based waveguide crossings," *Opt. Express*, vol. 16, pp. 8649–8657, 2008.
- [10] N. Sherwood-Droz, H. Wang, L. Chen, B. G. Lee, A. Biberman, K. Bergman, and M. Lipson, "Optical  $4 \times 4$  hitless silicon router for optical networks-on-chip (NoC)," *Opt. Express*, vol. 16, pp. 15915–15922, 2008.
- [11] B. E. Little and S. T. Chu, "Microring resonators for very large scale integrated photonics," in *Proc. Lasers and Electro-Optics Society 1999 12th Annual Meeting LEOS'99. IEEE*, 1999, vol. 2, pp. 487–488.
- [12] E. J. Klein, D. H. Geuzebroek, H. Kelderman, G. Sengo, N. Baker, and A. Driessen, "Reconfigurable optical add-drop multiplexer using microring resonators," *IEEE Photonic Tech. Lett.*, vol. 17, no. 11, pp. 2358–2360, Nov. 2005.
- [13] E. Drouard, M. Briere, F. Mieyeville, I. O'Connor, X. Letartre, and F. Gaffiot, "Optical network on chip multidomain modeling using syst-semc," in *Proc. 2004 Forum on Specification and Design Languages*, Lille, France, 2004.
- [14] W. Bogaerts, P. Dumon, D. Van Thourhout, and R. Baets, "Low-loss, low-crosstalk crossings for SOI Nanophotonic waveguides," *Opt. Lett.*, vol. 32, no. 19, pp. 2801–2803, 2007.
- [15] P. Dumon, W. Bogaerts, D. Van Thourhout, D. Taillaert, R. Baets, J. Wouters, S. Beckx, and P. Jaenen, "Compact wavelength router based on a silicon-on-insulator arrayed waveguide grating pigtailed to a fiber array," *Opt. Express*, vol. 14, no. 2, pp. 664–669, 2006.
- [16] W. Bogaerts, R. Baets, P. Dumon, V. Wiaux, S. Beckx, D. Taillaert, B. Luyssaert, J. Van Campenhout, P. Bienstman, and D. Van Thourhout, "Nanophotonic waveguides in silicon-on-insulator fabricated with CMOS technology," *J. Lightw. Technol.*, vol. 23, no. 1, pp. 401–412, 2005 (invited).
- [17] D. Taillaert, F. Van Laere, M. Ayre, W. Bogaerts, D. Van Thourhout, P. Bienstman, and R. Baets, "Grating couplers for coupling between optical fibers and Nanophotonic waveguides," *Jpn. J Appl. Phys.*, vol. 45, no. 8A, pp. 6071–6077, 2006.



**Andrzej Kaźmierczak** graduated (hons) from the Technical University, Lodź, Lodź (Poland), in 2003. He conducted his Ph.D. research at the T. U. Lodź (Poland) and at Ecole Centrale de Lyon, Ecully (France), obtaining Ph.D. degree in 2007.

He is currently an R&D engineer Multitel a.s.b.l., Mons, Belgium, where he is coordinating Multitel activities in SABIO (Ultrahigh sensitivity Slot-waveguide BIOsensor on a highly integrated chip for simultaneous diagnosis of multiple diseases) EU-founded project. His scientific interests include

integrated passive and active photonics devices and optical sensors. He is an author or coauthor of about 30 scientific communications published in journals and presented at international conferences. .



**Wim Bogaerts** (S'98–M'05) received the degree in engineering (applied physics) from Ghent University, Belgium, in 1998, and the Ph.D. degree from the Department of Information Technology (INTEC) at both Ghent University and the Interuniversity Microelectronics Center (IMEC), Leuven, Belgium, in 2004.

In the photonics research group he specialized in modeling, design, and fabrication of nanophotonic components. He is currently a Postdoctoral Fellow at the Flemish Research Foundation (FWO-Vlaanderen) and coordinates the fabrication

of nanophotonic components in SOI in IMEC, as a part of the European Network of Excellence ePIXnet.

Dr. Bogaerts is a member of the IEEE-Laser and Electro-Optics Society and Optical Society of America.

**Emmanuel Drouard** received the Ph.D. degree from the University of Aix-Marseille III, France, in 2003, on the design and experimental study of integrated optics devices made by Ti ion implantation in silica.

In 2003, he joined LEOM (now INL). He is currently an Associate Professor at the Ecole Centrale de Lyon, Ecully, France. His current research interests include the modeling and simulation of integrated optics refractive and diffractive devices for optical interconnects.

**Fabian Dortu** received the M.Sc. degree in physical engineering from the Université de Liège, Liège, Belgium, in 2001. He is currently working toward the Ph.D. degree at the Katholieke Universiteit Leuven, Leuven, Belgium in collaboration with the Interuniversity Micro-Electronics Centre (IMEC), Leuven, on the development of optical methods for the characterization of ultrashallow junctions.

He is currently with the Department of Applied Photonics at Multitel (Mons). His current research interests include the simulation and modeling of nonlinear effects in light semiconductor interaction, planar photonics, and fiber Bragg gratings.



**Pedro Rojo-Romeo** was born in 1958 in Madrid, Spain. He received the InG. Dipl. degree in physics in 1981 from the Institut National des Sciences Appliquées (INSA), Lyon, France, in 1981, and the Ph.D. degree in electronic devices from the INSA, Lyon, in 1984.

Since 1988, he has been an Associate Professor of electronics at the Ecole Centrale de Lyon, Ecully Cedex, France, Institute of Nanotechnologies of Lyon (INL), Ecully, France. His current research interests include electrical and optical devices

fabrication technology, characterization of microelectronic and optoelectronic micro nanodevices. He is also involved in optical interconnection systems, nanotechnologies, and optical integrated circuits technologies. His recent research areas are focused on heterogeneous integration of III-V structures on Si-based substrates; development of CMOS compatible III-V nanolasers coupled to Si waveguides (programs FP6-STREP-PICMOS, FP7-STREP-WADIMOS, French program RMNT HETEROPT), development of novel 2.5-D photonic crystal lasers for guided and free-space laser emission (French program PNANO HEVICAL, FP7-PI-HELIOS), localization of nanostructures on a patterned surface using e-beam lithography techniques; localization of InAs quantum dots on InP for single photon sources (French program NANOQUB), localized growth of III V nanowires on Si.

**Frederic Gaffiot**, photograph and biography not available at the time of publication.



**Dries Van Thourhout** received the degree in physical engineering and the Ph.D. degree from Ghent University, Ghent, Belgium, in 1995 and 2000, respectively.

From October 2000 to September 2002, he was with Lucent Technologies, Bell Laboratories, New Providence, NJ, where he was engaged in the design, processing, and characterization of InP/InGaAsP monolithically integrated devices. In October 2002, he joined the Department of Information Technology (INTEC), Ghent University, where he is currently a

member of the permanent staff of the Photonics Group and is also a Lecturer or a Colecturer for four courses within the Ghent University Master in Photonics program (Microphotonics, Advanced Photonics Laboratory, Photonic Semiconductor Components and Technology). He is also coordinating the cleanroom activities of the research group. His current research interests include the design, fabrication, and characterization of integrated photonic devices, including silicon nanophotonic devices, heterogeneous integration of InP-on-silicon, and integrated InP-based optical isolators. He is also engaged in research on the development of new fabrication processes for photonic devices, e.g., based on focused ion beam etching and die-to-wafer bonding. He has authored and coauthored over 60 journal papers, and has presented invited papers at several major conferences.

Dr. Thourhout is a member of the IEEE-Laser and Electro-Optics Society and an Associate Editor for the IEEE PHOTONICS TECHNOLOGY LETTERS.

**Domenico Giannone** received the Ph.D. degree with the Photonics Research Group, Aston University, Birmingham, U.K. He was involved on several aspects of fibre Bragg grating technology. He was with the British Telecom Laboratories (U.K.).

Since 2003, he has been with the Applied Photonics Department, Multitel. He is author and coauthor of more than 20 journal and conference papers on fibre lasers and fibre Bragg grating technology.